Published in final edited form as:
J Orthop Res. 2012 February ; 30(2): 288–295. doi:10.1002/jor.21501.

Inhibin A enhances bone formation during distraction osteogenesis

Daniel S. Perrien[1,3], **Kristy M. Nicks**[1,4], **Lichu Liu**[2], **Nisreen S. Akel**[1], **Anthony W. Bacon**[2], **Robert A. Skinner**[2], **Frances L. Swain**[2], **James Aronson**[2], **Larry J Suva**[1,2], and **Dana Gaddy**[1,2,*]

[1]Department of Physiology and Biophysics, University of Arkansas for Medical Sciences, 4301 W. Markham, Slot 505, Little Rock, AR 72205

[2]Center for Orthopaedic Research, Department of Orthopaedic Surgery, University of Arkansas for Medical Sciences, 4301 W. Markham, Slot 644, Little Rock, AR 72205

Abstract

Given the aging population and the increased incidence of fracture in the elderly population, the need exists for agents that can enhance bone healing, particularly in situations of delayed fracture healing and/or non-union. Our previous studies demonstrated that over-expression of the gonadal peptide, human Inhibin A (hInhA), in transgenic mice enhances bone formation and strength via increased osteoblast activity. We tested the hypothesis that hInhA can also exert anabolic effects in a murine model of distraction osteogenesis (DO), using both transgenic hInhA overexpression and administration of normal physiological levels of hInhA in adult male Swiss-Webster mice. Tibial osteotomies and external ring fixation were performed, followed by a 3 day latency period, 14 day distraction, and sacrifice on day 18. Supraphysiological levels of hInhA in transgenic mice, but not normal physiological levels of hInhA, significantly increased endosteal bone formation and mineralized bone area in the distraction gap, as determined by radiographic and μCT analysis. Significantly, increased PCNA and osteocalcin expression in the primary matrix front suggested that hInhA increased osteoblast proliferation. This mechanism is consistent with the effects of other agents and pathologies that modulate bone formation during DO, and demonstrates the potential of hInhA to enhance bone repair and regeneration.

Keywords

Inhibin; anabolism; distraction osteogenesis; bone formation; bone repair

Introduction

Non-steroidal hormones in the hypothalamic-pituitary-gonadal skeletal (HPGS) axis are part of the repertoire of endocrine hormones regulating skeletal metabolism (1–5). We have demonstrated that Inhibins regulate osteoblast and osteoclast differentiation in mouse and human cells 6, 7 and that changes in Inhibins, independent of changes in estradiol or follicle

[*]**Send reprint requests to:** Dana Gaddy, Ph.D., University of Arkansas for Medical Sciences, 4301 W. Markham, Slot 505, Little Rock, AR 72205, 501-686-5918, 501-686-8167 FAX, gaddydana@uams.edu.
[3]**Current Address:** Department of Orthopaedics & Rehabilitation, Vanderbilt Center for Bone Biology, and Vanderbilt University Institute for Imaging Sciences, Medical Center East, South Tower, Suite 4200, Nashville, TN 37232-8774
[4]**Current Address:** Division of Endocrinology, Diabetes, Metabolism and Nutrition, Mayo Clinic, Guggenheim 7, 200 First Street SW, Rochester, MN 55905

The authors have no professional or financial affiliations to disclose.

stimulating hormone (FSH), lead to changes in bone turnover (8). Using a transgenic mouse model of inducible Inhibin A (InhA) overexpression that produces serum InhA concentrations of 400–800 pg/ml (9), we have also demonstrated skeletal anabolism of InhA. Continuous exposure to these levels of InhA stimulates increases in trabecular bone mass, architecture and strength in both the tibia and spine, primarily via increases in osteoblast activity (6).

To gain additional insight into the mechanistic basis of Inhibin's stimulatory effects on bone formation and to determine whether it has a similar anabolic affect during bone regeneration, we utilized a uniquely suitable model of cellular organization and isolation of osteoblastogenesis offered by the distraction osteogenesis (DO) process (10, 11). Our study was focused in the early stages of DO, when osteoblast proliferation and differentiation predominate and did not include the later stages of DO repair and consolidation (10, 11). We hypothesized that the effect of InhA overexpression would be similar to that seen in intact animals, namely that InhA would be anabolic and accelerate the amount of bone formed during the distraction period and that other mechanisms would potentially control consolidation. Thus, DO was performed on adult male *Glvp/InhA* mice implanted with mifepristone (MFP) pellets to induce InhA overexpression or treated with vehicle pellets alone, as we have previously described (6), to determine the effect of InhA overexpression on bone regeneration during DO. In a second study, we tested the idea that physiological InhA concentrations (30–80 pg/ml) would also be sufficient to achieve anabolic effects during DO. We administered human InhA at a dose of 30–80 pg/ml, via osmotic mini pump, initiated at the time of osteotomy and continuing through the 14 days of distraction in male Swiss Webster mice at peak adult bone mass.

We show here that InhA was dramatically anabolic and accelerated the amount of new bone formation during DO when mice were exposed to InhA overexpression, but not when exposed to normal physiological InhA levels.

Materials

Animals and Reagents

An inducible InhA bigenic transgenic mouse line (6), $Glvp^{+/+}:hInhA^{+/-}$ (Glvp/InhA) were gifted by Dr. Teresa Woodruff (Northwestern University, Evanston, IL) and the colony developed to utilize mice at peak adult bone mass for their individual strain (4.5 months of age) (6). Normal Swiss Webster mice at adult peak bone mass, aged 3–4 months, were purchased from Jackson Laboratory (Bar Harbor, ME). Controlled release pellets for subcutaneous delivery of either vehicle (Veh group) or 6 micrograms per day of mifipristone (MFP; Glvp/InhA group) to induce continuous InhA overexpression in Glvp/InhA mice were purchased from Innovative Research of America, Toledo, OH (6). Analytical grade reagents were purchased from Sigma (St. Louis, MO), and antibodies for immunofluorescence were purchased from Cell Signaling (Boston, MA). Recombinant human Inhibin A and human-specific InhA ELISAs were purchased from Diagnostic Systems Laboratories (Webster, TX).

Osteotomies and Distraction Osteogenesis

The Institutional Animal Care and Use Committee (IACUC) of the University of Arkansas for Medical Sciences approved all animal procedures. Under deep xylazine/ketamine anesthesia each mouse was fitted with a full ring external fixator on the left tibia as described previously (10, 12). Transgenic mice were then implanted s.c. with either vehicle pellet or MFP to deliver 3.2 μg/day hInhA (6). Swiss-Webster mice were implanted s.c. with Alzet minipumps containing human InhA in 0.1% BSA/0.1N Acetic Acid that was

calculated to generate serum levels of 30–80 pg/ml/day delivery of InhA for 21 days. Control pumps contained vehicle only. Finally, all mice received an intramuscular injection of buprenorphine (1.0 mg/kg) for analgesia, and were observation during recovery. All animals tolerated and adapted well to the fixated leg as indicated by normal ambulation and weight bearing on the leg by 48 hr post-surgery. Distraction was initiated 3 days after surgery (3-day latency) at a rate of 0.075 mm twice a day (0.15 mm/day) and continued for 14 days.

Following 14 days of distraction, all animals were sacrificed under xylazine/ketamine anesthesia (postoperative day 18). Distracted tibiae were removed by disarticulation at the knee and ankle and placed in 10% neutral buffered formalin with the external fixators in place. After fixation, soft tissues were dissected away, and the tibiae were removed from the fixators for high-resolution single-beam radiography, followed by microCT analysis and subsequent histological processing as we have described (10, 12–15).

Radiographic Analysis of Bone Formation During DO

A Xerox Micro 50 closed system radiography unit (Xerox, Pasadena, CA; 40 kV (3 mA) for 20 s) was used (10). Comparison of distraction gap radiodensities was made by videomicroscopy using NIH Image Analysis 1.49 (NIH, Bethesda, MD; http://rsb.info.nih.gov/nih-image/index.html). The measured distraction gap area was outlined from the outside corners of the two proximal and the two distal cortices forming a quadrilateral region of interest as we have described (10).

MicroCT Analysis of Regenerate Bone Formation in Distraction Osteogenesis

Following analytical radiography bone formation was analyzed using a μCT40 (Scanco Medical AG, Bassersdorf, Switzerland) and the manufacturer's software. The tibia including the entire distraction gap of was scanned in cross section with an isotropic voxel size of 12 μm at 55 kV, 114 μA, and 1000 projections per rotation. Endosteal gap volume was defined as the volume of a cylinder approximating the shape and volume of the marrow cavity between the proximal and distal ends of the host cortices. Endosteal new bone was defined as bone residing within the endosteal gap volume. At the proximal end of the DO gap, the endosteal surface of the host cortex was outlined in the last cross sectional image in which the cortex appeared intact. That specific outline was copied and pasted onto the slice in which ~50% of the host cortex is missing, defining the region of interest for that slice and the proximal end of the DO gap. This procedure was repeated for the distal end of the DO gap. The ROI for each of the interceding slices was defined by hand drawn contours to account for the significant changes in the size and position throughout the distraction gap.

For both the endosteal and periosteal analyses, bone was segmented from soft tissue by applying an optimized grey scale threshold and a 3-dimensional noise filter to create a binary 3-dimensional reconstruction. The threshold and noise filter used were the same as that used for the trabecular analysis of intact mouse bones (sigma 0.8, support 1, threshold 245) as we have described (6, 16). Total volume and bone volume were calculated directly from the sum of the individual voxel volumes in the 3-dimensional reconstruction. The bone volumes were normalized to total gap volume to yield a ratio of proximal new bone/gap volume or distal new bone/gap volume, respectively. These data are analogous to the 2-dimensional radiographic and histological measures that we have used previously (17, 18).

Histological Analysis of New Bone Matrix

After radiography and μCT imaging, the distracted tibiae were decalcified in 5% formic acid, paraffin-embedded and longitudinal 5–7μm sections obtained and stained with hematoxylin and eosin (H&E). The sections chosen for analysis represented a central or near

central distraction gap location. Endosteal new bone was defined as that arising from the marrow space between the host cortices as previously described (12, 13, 19–21). For histological quantification of DO gap matrix formation, a digital image of each slide was captured under low-power (2× objective) microscopic magnification and analyzed using NIH Image. The distraction gap area was outlined from the outside corners of the two proximal and the two distal cortices forming a quadrilateral region of interest, and the area of that region (gap area) was recorded. Both the proximal (PNB) and distal endosteal new bone (DNB) matrix, which is easily distinguished from the central fibrous tissue at the primary matrix front, was outlined and the area recorded. The percentage of new bone area within the distraction gap was calculated by dividing bone matrix area by gap area (13–15, 22, 23), and osteocyte number per endosteal new bone area was enumerated as a measure of cellularity in the endosteal new bone. Proliferating cell nuclear antigen (PCNA) staining was performed on decalcified tissue with the FL-261 rabbit anti-mouse PCNA (1:100 dilution in PBS), followed by biotinylated goat anti-rabbit secondary antibody, then incubation with horseradish peroxidase–streptavidin followed by color development with NovaRed (Vector Laboratories, Burlingame, CA) and counterstained with Harris' hematoxylin (10). The number of PCNA positive cells adjacent to the endosteal new bone (ENB) were quantified in four 20× light field microscopic visual fields across the proximal PMF of each slide for each sample. Similarly, osteocalcin staining of the PMF was performed on decalcified, deparaffinized sections using a murine osteocalcin specific rabbit anti-mouse antibody (Enzo Life Sciences) at 1:8000 dilution overnight at 4C followed by incubation with rabbit horseradish peroxidase, and counterstained with Harris' Hematoxylin (10).

Human-Specific Serum Inhibin A Assay

Human-specific InhA was measured by a 2-site ELISA according to manufacturer's protocol as described previously (6). Blood was collected at sacrifice by cardiac puncture, allowed to clot on ice for 1 hr, and serum obtained. The detection limit of human InhA is <10 pg/ml, and intra-assay variability < 10% CV.

Statistical Analysis

Student's t-test was used to analyze data that passed normalization tests for these studies. A p-value of <0.05 was considered statistically significant between the 2 groups.

Results

The concentration of human InhA was measured in serum collected at sacrifice to confirm systemic hInhA levels in Swiss-Webster mice treated with hInhA (Figure 1A) and to determine the extent of MFP-induced hInhA overexpression in transgenic animals (Figure 1B). The mean serum hInhA concentration in Swiss-Webster mice was in the normal physiological range of 30–80 pg/ml (Figure 1A), whereas serum hInhA levels in Glvp/InhA transgenic mice were more than 10-fold higher (200–800 pg/ml) than the normal physiological range (Figure 1B).

Standard 2-dimensional radiographic methods were used to examine the effects of InhA on endosteal mineralized bone formation (that arising from between the host cortices) in the distraction gap. Analysis revealed that treatment with normal physiological levels of hInhA did not significantly affect endosteal new bone formation in the distraction gap (Figure 2A). However, supraphysiologic overexpression of hInhA during the distraction period significantly increased the percentage of the distraction gap occupied by new mineralized bone (Figure 2B).

Histologically, three zones of bone formation are defined within the distraction gap. 1) the fibrous interzone (FIZ) located in the middle of the gap and filled with fibroblastic cells within parallel collagen bundles; 2) the primary matrix front (PMF) located on both borders of the fibrous interzone and where cell proliferation and new osteoid deposition occurs; and 3) the zone of microcolumn formation (MCF) where the osteoblasts become embedded in parallel mineralized bone columns (10, 13, 24). The MCF zone containing endosteal new bone was observed in Glvp/InhA mice treated with vehicle and overexpressing InhA (Figure 3A and 3B).

The area of new bone matrix formed in the distraction gap was also measured in central histological sections of the distracted tibiae as described (10, 13, 24). InhA overexpression in Glvp/InhA mice did not affect the total amount of new bone matrix formed in the endosteal DO gap (Figure 3C). Despite the lack of effect on the PMF, InhA overexpression in Glvp/InhA mice significantly increased new mineralized bone formation (Figures 2 and 4).

To obtain a more comprehensive and higher resolution measure of mineralized bone in the total endosteal distraction gap, the distracted bones were analyzed utilizing μCT (12, 14, 25, 26). The treatment of Swiss-Webster mice with normal physiological levels of InhA for 18 days did not enhance n new bone formation in the DO gap (Figure 4A). However, consistent with the results of the standard 2D radiographic analysis in Glvp/InhA mice (Figure 2), analysis by μCT demonstrated that InhA overexpressing Glvp/InhA mice had significantly more endosteal regenerate bone compared to Vehicle treated mice (Figure 4A, B). Since a threshold equal to that used for the evaluation of mature trabecular bone was used, this result suggests that InhA overexpression accelerates the formation of mature mineralized bone during bone healing.

Next, the proliferation of osteoblasts in the primary matrix front of InhA overexpressing Glvp/InhA mice was examined by immunohistochemical staining for PCNA expression (Figure 5). Enumeration of the numbers of proliferating cells demonstrated significantly increased numbers of proliferating cells in the PMF of InhA over-expressing mice compared to Vehicle (Figure 5D). Staining of the osteoblast specific marker osteocalcin was used to confirm that proliferating cells were indeed osteoblastic lineage cells (Figure 6). InhA stimulated proliferating cells of the osteoblastic lineage (Figure 6B) indicating that the InhA stimulated increase in bone formation during DO is mediated by increased proliferation of osteoblasts. Importantly, this observation does not exclude other potential InhA effects on osteoblast differentiation and activity. This is consistent with our previous findings in intact and gonadectomized Glvp/InhA mice in which the targets of InhA anabolism were also cells of the osteoblast lineage (6).

Discussion

Our previous results demonstrated that InhA overexpression increases bone formation by stimulating mature osteoblast activity (6). Based on those observations the current study tested whether InhA treatment, either via transgenic over-expression or via osmotic minipump administration of normal physiological levels of InhA, increases bone formation during DO. Analysis using both 2-dimensional soft radiography (Figure 2) and 3-dimensional μCT (Figure 4) demonstrated that whereas normal physiological levels of InhA were insufficient to stimulate bone formation during DO, transgenic InhA overexpression significantly increased the volume of mineralized endosteal bone formed during the distraction protocol. In contrast, analysis of histological sections of distraction gaps from the same study (Figure 3) did not find that InhA overexpression significantly increased the area of bone matrix in the endosteal distraction gap.

The consistent increase in mineralized bone without a change in bone matrix area suggests that Inhibin increases the rate at which bone matrix is mineralized rather than affecting matrix synthesis and mineralization equally. Bone formation during DO is so rapid that osteoblasts must continue to mineralize the matrix, often after being embedded in the matrix.

Our current understanding is that osteoblastogenesis is characterized by at least three primary stages, proliferation, extracellular matrix maturation and mineralization (27–29), although recent observations raise the intriguing idea that these specific osteoblast differentiation stages may be controlled separately (30, 31–34). For example, expression of the protein convertase SKI-1 controls initiation of osteoblastic mineralization, without affecting proliferation (30). Collectively, our data support the idea that the regulation of osteoblast proliferation and activity can be separated and suggest that InhA treatment can activate proliferation and mineralization without effects on matrix production. These InhA-mediated increases in the activity of mature osteoblasts (mineralization) are consistent with our previous findings (6).

While differences in the results of the histological versus radiographic and μCT analysis of endosteal bone area suggest selective effects of InhA overexpression on mineralization, the results of the immunohistochemical staining for PCNA expression suggest that InhA also significantly increases osteoblast proliferation, at least in the primary matrix front (Figure 5D). These observations are consistent with the ability of *in vivo* InhA overexpression to stimulate *ex vivo* osteoblastogenesis (6), and would lead to both increases in the number of matrix-producing osteoblasts, as well as increases in their activity, as measured by the rate of mineralization. Such a mechanism is consistent with the effects of other several other agents and pathologies during DO (12, 13, 22, 25, 35–38), and thus is a likely mechanism to accelerate repair and regeneration.

Additional studies are necessary to further elucidate the potential mechanisms of InhA anabolism during DO. A preferential increase in matrix mineralization could be detected by measuring the mineralization lag time or measuring material properties of the matrix by spectroscopy in the distraction gap. However, these measurements require the use of non-decalcified sections, and the analytical procedures used in this study precluded this analysis since the sections were decalcified in formic acid. DO is uniquely suited to quantify the function of primarily osteoblasts during bone formation in vivo. We propose that the results described here provide novel insight into bone growth and bone healing. The effects of InhA on bone consolidation after DO remain unstudied and are the focus of current investigation.

Although normal physiological levels of systemic InhA do not enhance bone formation in the distraction gap, supraphysiological levels of InhA accelerate bone repair during DO via mechanisms involving enhanced osteoblastic proliferation and mineralization. Finally, these studies identify InhA and its signaling pathway as a novel therapeutic target to enhance bone repair in a variety of clinical settings. Further studies are underway to elucidate the dose-response for the observed InhA effects, and to identify the specific molecular target(s) of the stimulatory effects InhA action on osteoblastic proliferation and mineralization.

Acknowledgments

Funded by NIH R01-54044, NIH R21-74024, Musculoskeletal Transplant Foundation research grant to DG; NIH F31-DK079362 to KMN; NASA Graduate Student Research Program grant NNG04GP39H to DP; Carl L Nelson Endowed Chair in Orthopaedic Creativity to LJS.

References

1. Ebeling PR, Atley LM, Guthrie JR, Burger HG, Dennerstein L, Hopper JL, Wark JD. Bone turnover markers and bone density across the menopausal transition. J Clin Endocrinol Metab. 1996; 81:3366–3371. [PubMed: 8784098]
2. Vural F, Vural B, Yucesoy I, Badur S. Ovarian aging and bone metabolism in menstruating women aged 35–50 years. Maturitas. 2005; 52:147–153. [PubMed: 16186077]
3. Guthrie JR, Ebeling PR, Hopper JL, Dennerstein L, Wark JD, Burger HG. Bone mineral density and hormone levels in menopausal Australian women. Gynecol Endocrinol. 1996; 10:199–205. [PubMed: 8862496]
4. Sun L, Peng Y, Sharrow AC, Iqbal J, Zhang Z, Papachristou DJ, Zaidi S, Zhu LL, Yaroslavskiy BB, Zhou H, Zallone A, Sairam MR, Kumar TR, Bo W, Braun J, Cardoso-Landa L, Schaffler MB, Moonga BS, Blair HC, Zaidi M. FSH directly regulates bone mass. Cell. 2006; 125:247–260. [PubMed: 16630814]
5. Nicks KM, Fowler TW, Gaddy D. Reproductive hormones and bone. Curr Osteoporos Rep. 2010; 8:60–67. [PubMed: 20425612]
6. Perrien DS, Akel NS, Edwards PK, Carver AA, Bendre MS, Swain FL, Skinner RA, Hogue WR, Nicks KM, Pierson TM, Suva LJ, Gaddy D. Inhibin A is an endocrine stimulator of bone mass and strength. Endocrinology. 2007; 148:1654–1665. [PubMed: 17194739]
7. Gaddy-Kurten D, Coker JK, Abe E, Jilka RL, Manolagas SC. Inhibin suppresses and activin stimulates osteoblastogenesis and osteoclastogenesis in murine bone marrow cultures. Endocrinology. 2002; 143:74–83. [PubMed: 11751595]
8. Perrien DS, Achenbach SJ, Bledsoe SE, Walser B, Suva LJ, Khosla S, Gaddy D. Bone turnover across the menopause transition: correlations with inhibins and follicle-stimulating hormone. J Clin Endocrinol Metab. 2006; 91:1848–1854. [PubMed: 16449331]
9. Pierson TM, Wang Y, DeMayo FJ, Matzuk MM, Tsai SY, Omalley BW. Regulable expression of inhibin A in wild-type and inhibin alpha null mice. Mol Endocrinol. 2000; 14:1075–1085. [PubMed: 10894156]
10. Aronson J, Liu L, Liu Z, Gao GG, Perrien DS, Brown EC, Skinner RA, Thomas JR, Morris KD, Suva LJ, Badger TM, Lumpkin CK. Decreased endosteal intramembranous bone formation accompanies aging in a mouse model of distraction osteogenesis. The Journal of Regenerative Medicine. 2002; 3:7–16.
11. Aronson J, Shen XC, Skinner RA, Hogue WR, Badger TM, Lumpkin CK Jr. Rat model of distraction osteogenesis. J Orthop Res. 1997; 15:221–226. [PubMed: 9167624]
12. Thrailkill KM, Liu L, Wahl EC, Bunn RC, Perrien DS, Cockrell GE, Skinner RA, Hogue WR, Carver AA, Fowlkes JL, Aronson J, Lumpkin CK Jr. Bone formation is impaired in a model of type 1 diabetes. Diabetes. 2005; 54:2875–2881. [PubMed: 16186388]
13. Wahl EC, Aronson J, Liu L, Skinner RA, Miller MJ, Cockrell GE, Fowlkes JL, Thrailkill KM, Bunn RC, Ronis MJ, Lumpkin CK Jr. Direct bone formation during distraction osteogenesis does not require TNFalpha receptors and elevated serum TNFalpha fails to inhibit bone formation in TNFR1 deficient mice. Bone. 2010; 46:410–417. [PubMed: 19772956]
14. Wahl EC, Liu L, Perrien DS, Aronson J, Hogue WR, Skinner RA, Hidestrand M, Ronis MJ, Badger TM, Lumpkin CK Jr. A novel mouse model for the study of the inhibitory effects of chronic ethanol exposure on direct bone formation. Alcohol. 2006; 39:159–167. [PubMed: 17127135]
15. Wahl EC, Perrien DS, Aronson J, Liu Z, Fletcher TW, Skinner RA, Feige U, Suva LJ, Badger TM, Lumpkin CK Jr. Ethanol-induced inhibition of bone formation in a rat model of distraction osteogenesis: a role for the tumor necrosis factor signaling axis. Alcohol Clin Exp Res. 2005; 29:1466–1472. [PubMed: 16131855]
16. Suva LJ, Hartman E, Dilley JD, Russell S, Akel NS, Skinner RA, Hogue WR, Budde U, Varughese KI, Kanaji T, Ware J. Platelet dysfunction and a high bone mass phenotype in a murine model of platelet-type von Willebrand disease. Am J Pathol. 2008; 172:430–439. [PubMed: 18187573]

17. Ronis MJ, Aronson J, Gao GG, Hogue W, Skinner RA, Badger TM, Lumpkin CK Jr. Skeletal effects of developmental lead exposure in rats. Toxicol Sci. 2001; 62:321–329. [PubMed: 11452145]

18. Aronson J, Gao GG, Shen XC, McLaren SG, Skinner RA, Badger TM, Lumpkin CK Jr. The effect of aging on distraction osteogenesis in the rat. J Orthop Res. 2001; 19:421–427. [PubMed: 11398855]

19. Fowlkes JL, Thrailkill KM, Liu L, Wahl EC, Bunn RC, Cockrell GE, Perrien DS, Aronson J, Lumpkin CK Jr. Effects of systemic and local administration of recombinant human IGF-I (rhIGF-I) on de novo bone formation in an aged mouse model. J Bone Miner Res. 2006; 21:1359–1366. [PubMed: 16939394]

20. Ai-Aql ZS, Alagl AS, Graves DT, Gerstenfeld LC, Einhorn TA. Molecular mechanisms controlling bone formation during fracture healing and distraction osteogenesis. J Dent Res. 2008; 87:107–118. [PubMed: 18218835]

21. Jacobsen KA, Al-Aql ZS, Wan C, Fitch JL, Stapleton SN, Mason ZD, Cole RM, Gilbert SR, Clemens TL, Morgan EF, Einhorn TA, Gerstenfeld LC. Bone formation during distraction osteogenesis is dependent on both VEGFR1 and VEGFR2 signaling. J Bone Miner Res. 2008; 23:596–609. [PubMed: 18433297]

22. Wahl EC, Aronson J, Liu L, Liu Z, Perrien DS, Skinner RA, Badger TM, Ronis MJ, Lumpkin CK Jr. Chronic ethanol exposure inhibits distraction osteogenesis in a mouse model: role of the TNF signaling axis. Toxicol Appl Pharmacol. 2007; 220:302–310. [PubMed: 17391719]

23. Aronson J. Modulation of distraction osteogenesis in the aged rat by fibroblast growth factor. Clin Orthop Relat Res. 2004:264–283. [PubMed: 15292818]

24. Brown EC, Perrien DS, Fletcher TW, Irby DJ, Aronson J, Gao GG, Hogue WJ, Skinner RA, Suva LJ, Ronis MJ, Hakkak R, Badger TM, Lumpkin CK Jr. Skeletal toxicity associated with chronic ethanol exposure in a rat model using total enteral nutrition. J Pharmacol Exp Ther. 2002; 301:1132–1138. [PubMed: 12023547]

25. Haque T, Hamade F, Alam N, Kotsiopriftis M, Lauzier D, St-Arnaud R, Hamdy RC. Characterizing the BMP pathway in a wild type mouse model of distraction osteogenesis. Bone. 2008; 42:1144–1153. [PubMed: 18372226]

26. Fang TD, Nacamuli RP, Song HM, Fong KD, Warren SM, Salim A, Carano RA, Filvaroff EH, Longaker MT. Creation and characterization of a mouse model of mandibular distraction osteogenesis. Bone. 2004; 34:1004–1012. [PubMed: 15193546]

27. Friedenstein AJ, Petrakova KV, Kurolesova AI, Frolova GP. Heterotopic of bone marrow. Analysis of precursor cells for osteogenic and hematopoietic tissues. Transplantation. 1968; 6:230–247. [PubMed: 5654088]

28. Lian JB, Stein GS. Concepts of osteoblast growth and differentiation: basis for modulation of bone cell development and tissue formation. Crit Rev Oral Biol Med. 1992; 3:269–305. [PubMed: 1571474]

29. Aubin JE. Advances in the osteoblast lineage. Biochem Cell Biol. 1998; 76:899–910. [PubMed: 10392704]

30. Gorski JP, Huffman NT, Chittur S, Midura RJ, Black C, Oxford J, Seidah NG. Inhibition of proprotein convertase SKI-1 blocks transcription of key extracellular matrix genes regulating osteoblastic mineralization. J Biol Chem. 2011; 286:1836–1849. [PubMed: 21075843]

31. Morello R, Bertin TK, Chen Y, Hicks J, Tonachini L, Monticone M, Castagnola P, Rauch F, Glorieux FH, Vranka J, Bachinger HP, Pace JM, Schwarze U, Byers PH, Weis M, Fernandes RJ, Eyre DR, Yao Z, Boyce BF, Lee B. CRTAP is required for prolyl 3-hydroxylation and mutations cause recessive osteogenesis imperfecta. Cell. 2006; 127:291–304. [PubMed: 17055431]

32. Hoemann CD, El-Gabalawy H, McKee MD. In vitro osteogenesis assays: influence of the primary cell source on alkaline phosphatase activity and mineralization. Pathol Biol (Paris). 2009; 57:318–323. [PubMed: 18842361]

33. Murshed M, Harmey D, Millan JL, McKee MD, Karsenty G. Unique coexpression in osteoblasts of broadly expressed genes accounts for the spatial restriction of ECM mineralization to bone. Genes Dev. 2005; 19:1093–1104. [PubMed: 15833911]

34. Murshed M, Schinke T, McKee MD, Karsenty G. Extracellular matrix mineralization is regulated locally; different roles of two gla-containing proteins. J Cell Biol. 2004; 165:625–630. [PubMed: 15184399]

35. Perrien DS, Brown EC, Fletcher TW, Irby DJ, Aronson J, Gao GG, Skinner RA, Hogue WR, Feige U, Suva LJ, Ronis MJ, Badger TM, Lumpkin CK Jr. Interleukin-1 and tumor necrosis factor antagonists attenuate ethanol-induced inhibition of bone formation in a rat model of distraction osteogenesis. J Pharmacol Exp Ther. 2002; 303:904–908. [PubMed: 12438508]

36. Carvalho RS, Einhorn TA, Lehmann W, Edgar C, Al-Yamani A, Apazidis A, Pacicca D, Clemens TL, Gerstenfeld LC. The role of angiogenesis in a murine tibial model of distraction osteogenesis. Bone. 2004; 34:849–861. [PubMed: 15121017]

37. Amir LR, Li G, Schoenmaker T, Everts V, Bronckers AL. Effect of thrombin peptide 508 (TP508) on bone healing during distraction osteogenesis in rabbit tibia. Cell Tissue Res. 2007; 330:35–44. [PubMed: 17636332]

38. Cho TJ, Kim JA, Chung CY, Yoo WJ, Gerstenfeld LC, Einhorn TA, Choi IH. Expression and role of interleukin-6 in distraction osteogenesis. Calcif Tissue Int. 2007; 80:192–200. [PubMed: 17340223]

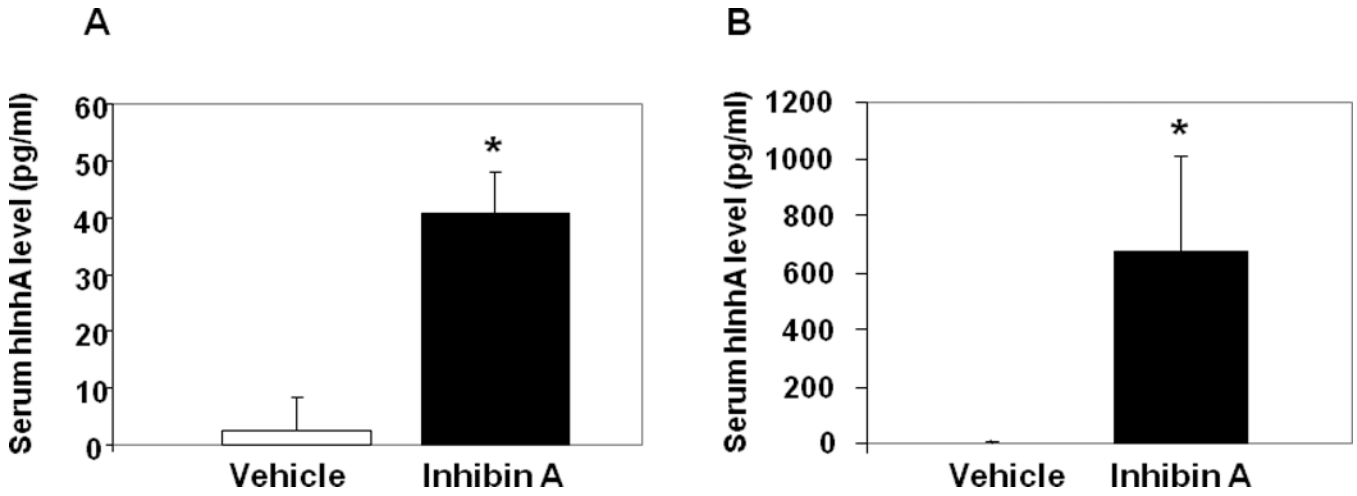

Figure 1. Serum hInhA levels are increased in vivo

(A) Normal Swiss-Webster mice treated with vehicle or hInhA (40.8+/−7.2 pg/ml) for 18 days. **(B)** Glvp/InhA bigenic mice were implanted with Vehicle or MFP to stimulate the systemic overexpression of hInhA. Human InhA was undetectable in both Swiss Webster **(A)** and Glvp/InhA mice treated with Vehicle **(B).** Data shown are mean +/− SD.;*=p<0.05.

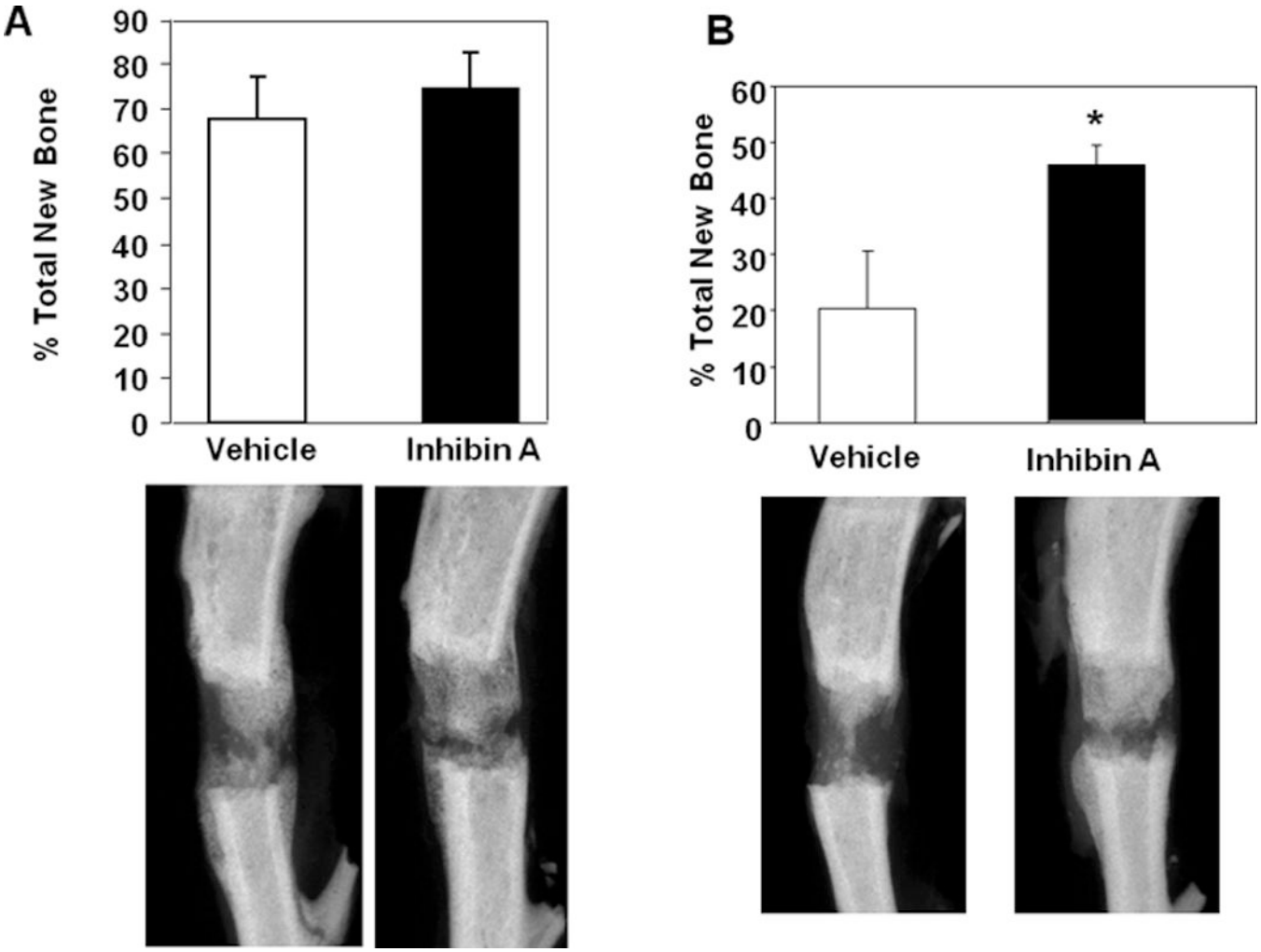

Figure 2. Supraphysiological concentrations of hInh A enhance new bone formation during DO

(Top) Percent total new bone area in the DO gap of **(A)** Swiss-Webster mouse tibiae treated with vehicle or physiological concentrations of hInhA by Alzet minipump for the 18 day duration of the experiment or **(B)** Glvp/InhA mice treated with Vehicle or MFP to overexpress InhA. Data shown are mean +/− SD; *=p<0.05. **(Bottom)** Representative X-ray images from each treatment are shown under the corresponding bars in the top panels.

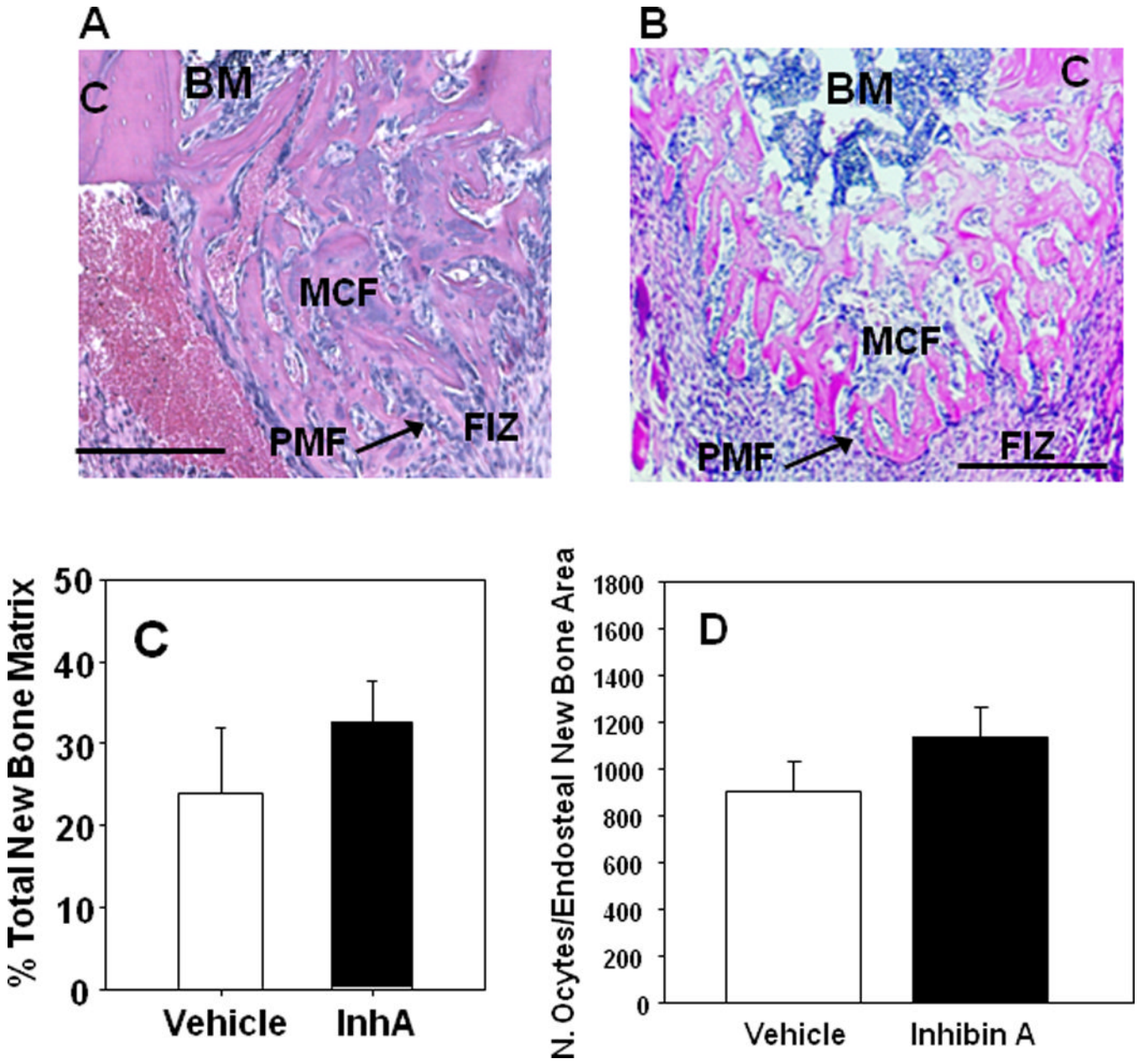

Figure 3. hInhA overexpression enhanced new microcolumn formation but not the area of new matrix formation during DO

Photomicrographs of the proximal half of a decalcified paraffin embedded histological sections of the DO gap in Glvp/InhA mice treated with Vehicle during DO **(A)**, or overexpressing hInhA during the time of DO **(B)** and stained with H&E depicting the major biological zones of the distraction gap. Analytically, the zone of microcolumn formation (MCF) is referred to as Endosteal New Bone (ENB). BM, Bone Marrow; C, Cortex; FIZ, Fibrous Interzone; PMF, Primary Matrix Front. Bars = 500μm. **(C)** The formation of new bone matrix in the endosteal distraction gap of Vehicle-treated Glvp/InhA mice and Glvp/InhA mice treated with MFP was assessed in central sections of decalcified DO gaps stained with H&E. (**D**) The osteocyte density in the ENB was enumerated per bone area in central

sections of decalcified DO gaps stained with H&E. No significant differences in cellularity were observed. Data shown are mean +/− SD.

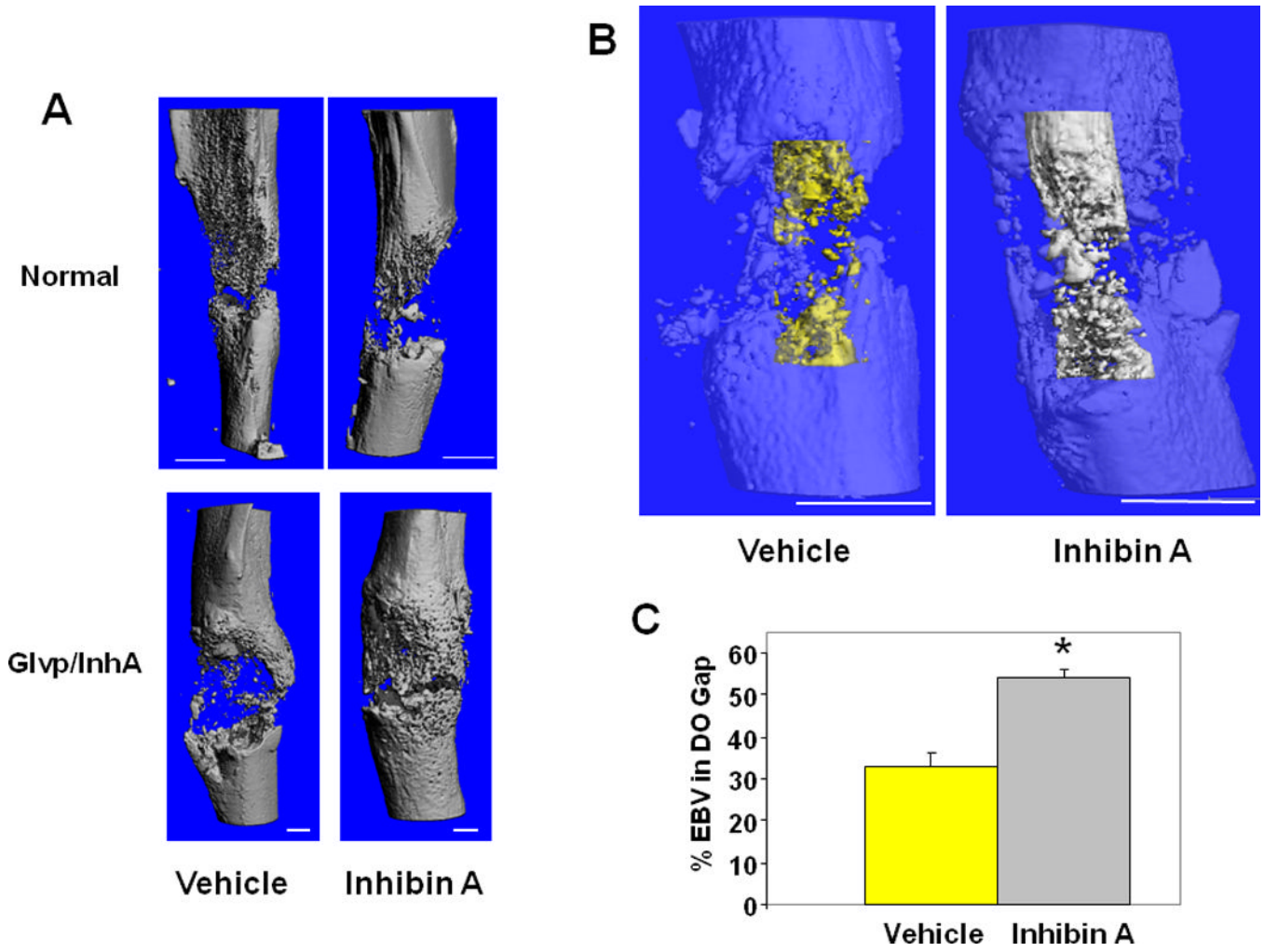

Figure 4. hInhA overexpression increases endosteal new bone formation during DO

(A) MicroCT reconstruction of mouse tibiae. **(Top)** Swiss-Webster treated with vehicle or hInhA for 18 days. **(Bottom)** Glvp/InhA mice treated with Vehicle or MFP to overexpress hInhA. Mice were sacrificed 18 days post-operatively and the DO gap scanned. **(B)** MicroCT translucent reconstructions illustrate hInhA effects on endosteal bone volume. 3-Dimensional reconstruction of endosteal new bone in Vehicle treated (yellow) and InhA overexpressing (gray) Glvp/InhA mice. **(C)** Total volume and bone volume of the endosteal distraction gap were calculated directly from the voxel volumes in the reconstruction. Data shown are mean +/− SD; *=P<0.05.

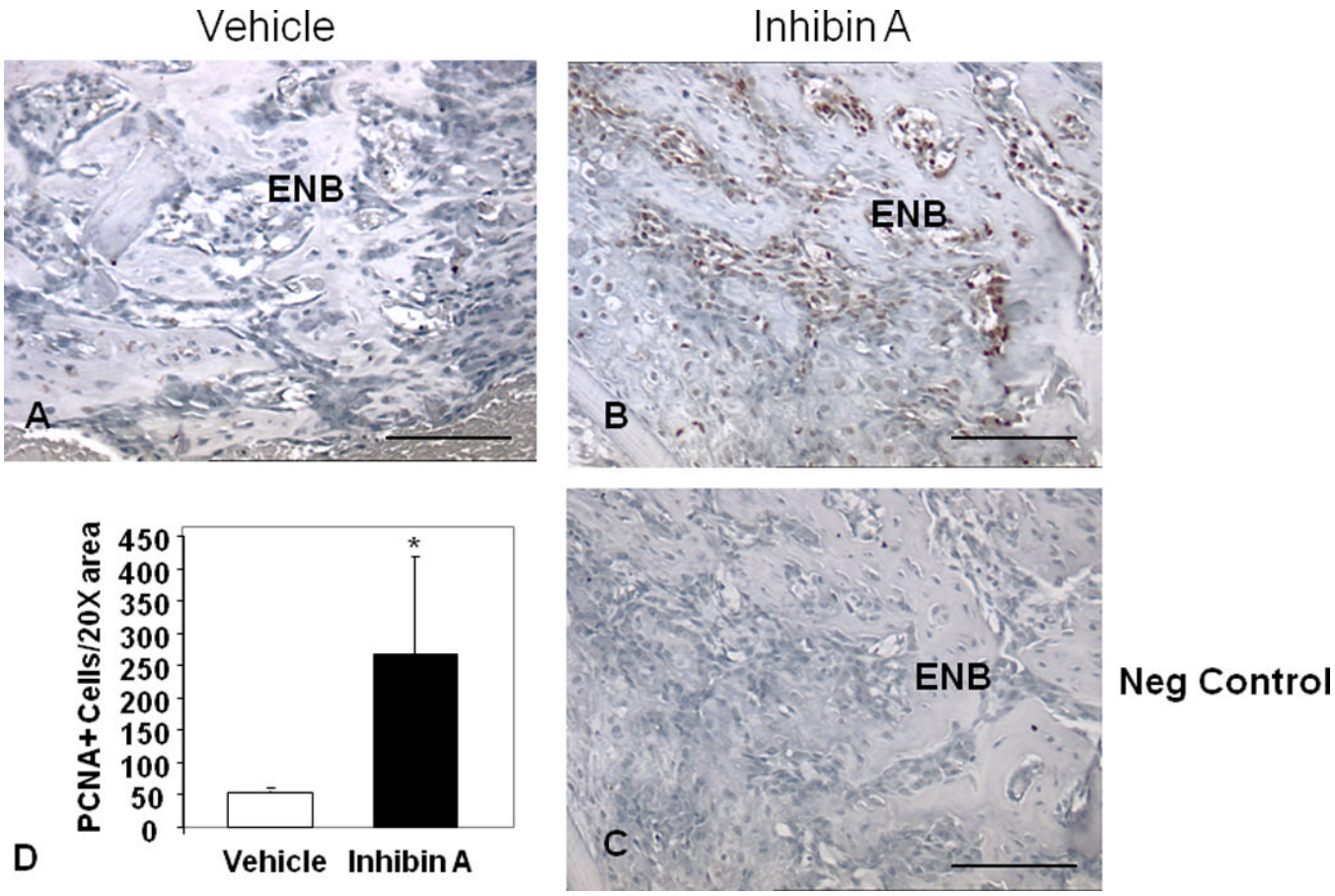

Figure 5. hInhA overexpression increases osteoblast proliferation in the primary matrix front (PMF) during DO

Paraffin embedded decalcified DO gaps containing ENB from Vehicle-treated Glvp/InhA mice and Glvp/InhA mice treated with MFP to stimulate hInhA overexpression (Glvp/InhA), stained for expression of proliferating cell nuclear antigen (PCNA, brown stain). (**A**) Vehicle treated, **(B, C)** hInhA overexpressing samples. (**C**) Negative control (no primary anti-PCNA antibody). Bars=500μm. **(D)** PCNA+ cells adjacent to the ENB were quantified in four 20× visual fields in the proximal PMF. Data are mean +/− SD; (*=P<0.05).

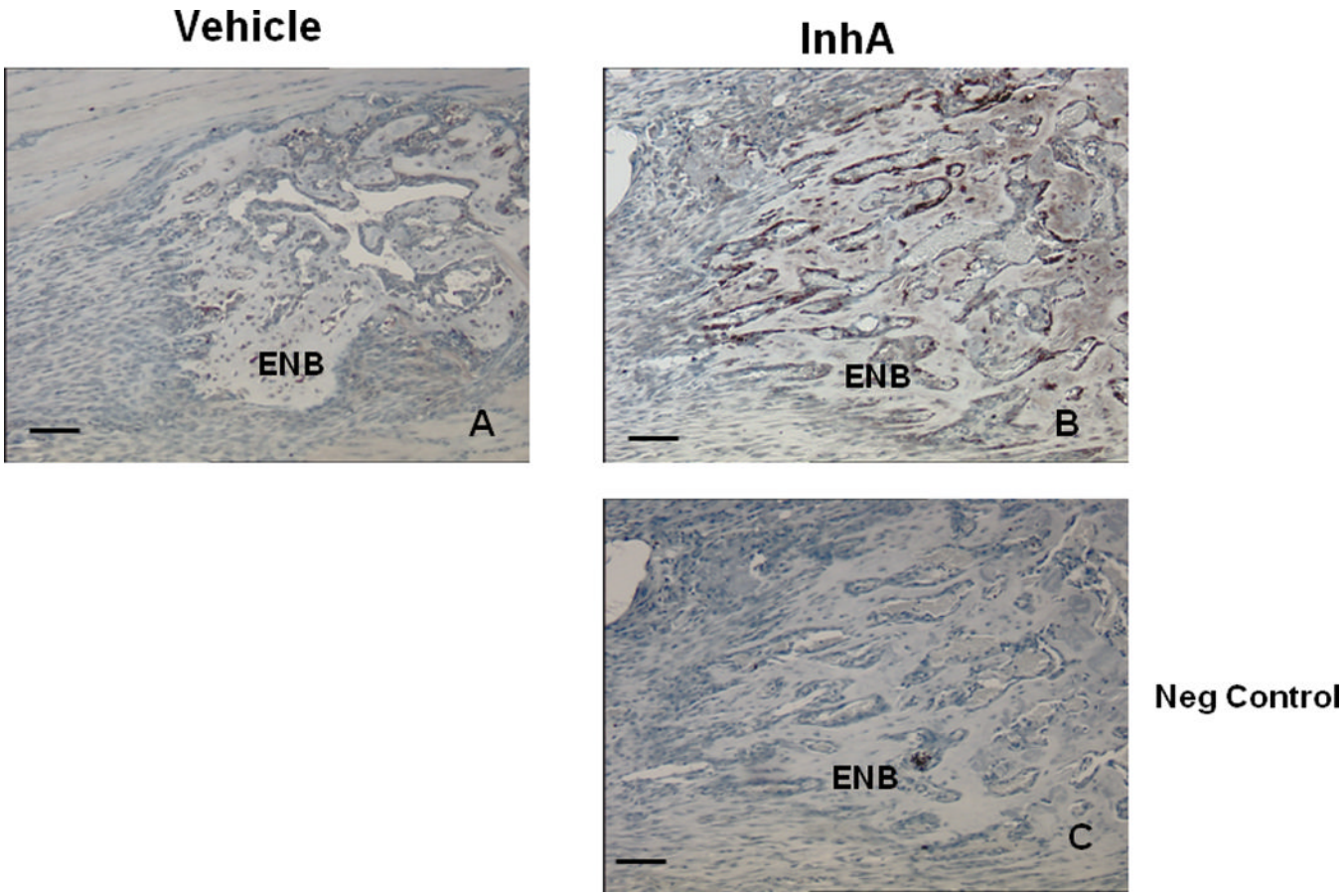

Figure 6. Osteocalcin expression identifies osteoblastic cells in the PMF during DO

Paraffin embedded decalcified DO gaps containing ENB from Vehicle-treated Glvp/InhA mice and Glvp/InhA mice treated with MFP to stimulate hInhA overexpression (Glvp/InhA), and stained for osteocalcin. (**A**) Vehicle treated, **(B, C)** InhA overexpressing samples. (**C**) Negative control (no primary anti-osteocalcin antibody) Bar=500μm.